IAI Accepts, published online ahead of print on 11 December 2006
Infect. Immun. doi:10.1128/IAI.00902-06

Functional characterization of the *Plasmodium* homologue of Macrophage Migration Inhibitory Factor (MIF)

Kevin D Augustijn[‡], Robert Kleemann[#], Joanne Thompson[§], Teake Kooistra[#], Carina E Crawford[§], Sarah E Reece[§], Arnab Pain[°], Arjan HG Siebum[+], Chris J Janse[‡] and Andrew P Waters[‡]*

Running title: *Plasmodium* encoded MIF homologue

[‡]*Department of Parasitology, LUMC, Albinusdreef 2, 2333 ZA, Leiden*

[#]*Vascular and Metabolic Diseases, TNO-Quality of Life, Zernikedreef 9,* 2333 CK, *Leiden*

[§]*Institute of Immunology and Infection Research, Kings Buildings, Ashworth Laboratories, West Mains Road, EH9 3JT, Edinburgh*

[°]*The Wellcome Trust Sanger Institute, Hinxton, Cambridge, CB10 1SA, Cambridge*

[+]*Leiden Institute of Chemistry, Gorlaeus Laboratories, Einsteinweg 55, 2333 CC, Leiden*

*To whom correspondence should be addressed: Department of Parasitology, LUMC, Albinusdreef 2, room P4-35, 2333 ZA, Leiden; Tel. +31-71 5265069; Fax. +31-71 5266907; E-mail: waters@lumc.nl.

Abstract

Macrophage migration inhibitory factor (MIF) is a mammalian cytokine that participates in innate and adaptive immune responses. Homologues of mammalian MIF have been discovered in parasite species infecting mammalian hosts (nematodes, malaria parasites), which suggests that these parasites express MIF to modulate the host immune response upon infection. We report the first biochemical and genetic characterization of a *Plasmodium* MIF (*P*MIF). Like human MIF, histidine tagged purified recombinant *P*MIF shows tautomerase and oxidoreductase activities (although reduced compared to histidine tagged human MIF) and efficiently inhibits AP-1 activity in human embryonic kidney cells. Furthermore, we demonstrate that *P.berghei* MIF is expressed in both mammalian host and mosquito vector and that, in blood stages, it is secreted into the infected erythrocyte and released upon schizont rupture. Mutant *P. berghei* parasites lacking *P*MIF were able to complete the entire life cycle and showed no significant changes in growth characteristics or virulence features during blood-stage infection. However, rodent hosts infected with knockout parasites had significantly higher numbers of circulating reticulocytes. Our results suggest that *P*MIF is produced by the parasite to influence host immune responses and the course of anaemia upon infection.

Introduction

Cytokines are the molecular messengers of the vertebrate immune system, coordinating the local and systemic immune responses to infective organisms. Macrophage Migration Inhibitory Factor (MIF) was one of the first cytokines to be discovered (4,17) and is involved in both innate and adaptive immune responses. MIF counter-regulates the anti-inflammatory effect of glucocorticoids (9) and is a key regulator of pro-inflammatory response to endotoxins. For example, MIF-deficient mice survive a lethal dose of lipopolysaccharide (LPS)(6). MIF is released by immune cells in response to microbial products and pro-inflammatory cytokines such as tumor necrosis factor α (10,12). While mammalian MIF is normally observed as a homomeric trimer, each subunit has two catalytic sites: a tautomerase activity, which requires an N-terminal proline residue (33) and an oxidoreductase activity (28), which is based on a thioredoxin-like motif. Although enzymatic activities are not normally found in cytokines, both of these activities have been linked to MIF's cytokine function (27,38,45). At the molecular level little is known about the exact mechanisms of MIF function; the biological substrate(s) for its enzymatic activities as well as its import and export pathways are not fully understood. So far, a classical cytokine receptor for MIF has not been discovered yet, and the surface receptor (CD74)(32) and the intracellular factor Jun activation domain binding protein (Jab-1)(27) are the only functional MIF-binding partners described.

Although the mode of action and the full biological role of host-derived MIF remain to be established, it has been shown that it also has a critical role in determining the outcome of infections caused by parasites such as helminths (42), malaria parasites (34) and *Leishmania* (44). Interestingly, homologues of human MIF (huMIF) have been characterized in nematodes (39,48,49). Parasitic nematodes are long-lived in their hosts and are able to modulate the immune response to evade killing by the immune system (reviewed in (26)). Therefore, it has been

suggested that the expression of MIF homologues plays a role in the immunobiology and immune evasion of these nematodes. In support of this, evidence has been found for a role of nematode MIF in activating macrophages and recruitment of eosinophils (20). Genome sequencing projects of other human parasites reveal that not only parasitic helminths, but also protozoa, such as *Plasmodium* contain genes encoding huMIF homologues(23). *Plasmodium* is the causative agent of malaria, which is responsible for over one million deaths annually and poses a tremendous social and economic burden (7). The potential ability of *Plasmodium* to manipulate the host-immune response though the secretion of cytokine homologues is clearly of interest.

In this study we report the first biochemical and genetic characterization of the *Plasmodium* homologues of MIF (*P*MIF) from two species, *P. falciparum* and *P. berghei*. We have demonstrated that C-terminal His_6 tagged *P*MIF exhibits similar biochemical and immune-stimulatory features as huMIF and that it is expressed during the blood-stages of parasite development in the mammalian host. Furthermore, gene deletion experiments showed that *Pb*MIF is not required for completion of the parasite life cycle but significantly influences the number of reticulocytes in the circulation of mice during the early stages of infection. Furthermore, we found that *P*MIF is secreted from infected red blood cells and ruptured schizonts. Coupled with the lack of an essential intracellular function, therefore, our data indicates that *P*MIF most likely has a function in the interaction of the parasite with its host.

Materials and methods

Plasmid construction. Protein expression constructs: MIF reading frames were amplified from mixed blood stage *P. falciparum* (Pf) (PlasmoDB entry *Pf*MIF: PFL1420w) and *P. berghei* (Pb) (GeneDB entry *Pb*MIF: PB000372.03.0) cDNA by PCR using the primers: L1632 5'-AAATTTCCGCATGCCGTGCTGTGAATTAATAAC-3', L1554 5'-ATTGGATCCACCAAATAGTGAGCCACTAAAAGC-3' (Pb) and L1667 5'-AAAATTTCCGCATGCCTTGCTGTGAAGTAATAAC-3', L1668 5'-ATTGGATCCGCCGAAAAGAGAACCACTGAAGGC-3' (Pf), digested (SphI, BamHI) and ligated into C-terminal His_6-tag expression vector pQE-70 (Qiagen). Genomic expression of GFP-tagged *Pb*MIF: the MIF gene and promoter region (1200 bp upstream sequence) were amplified from Pb genomic DNA using the primers: L1879 5'-AAAGGTATTCCATGGAACCAAATAGTGAGCCACTAAAAGCA-3' and L1880 5'-TAAATCAAAGCGGCCGCGAATCTTATCAACCATTTATACC-3', digested (NcoI, NotI) and ligated into the C-terminal GFP tagging integration construct, pGFP-TAG (30) or pMYC-TAG, which was generated by transferring the c-myc tag from pSD141 (41), a kind gift from Dr. Oliver Billker (Imperial College, London), into pGFP-TAG using the primers L2300 5'-CGGGGTACCGCGGCCGCTATCTAGACGAGGATCCATGGGGCCCGAACAAAAACTCATC-3' and L2301 5'- GAGCAGATTGTACTGAGAGTGCACCATATGCGGTG-3'. MIF knockout vector: upstream (-1200 to -300) and downstream regions (+785 to +1700) from the *pbmif* gene were amplified from Pb genomic DNA using the primers: L1466 5'-TAAATCAAGGTACCGGCGAATCTTATCAACCATTTATACC-3' L1467 5'-TTGTATTTCATCGATCTCTTGTGATATTAATCCATACACGCC-3' L1468 5'-AAAGAGGCTGAATTCTATGTAAATTATTTTTCCTATGCCCTTAAC-3' L1469

5'-ATCGGATCCTTATGCGTATATATATTGAAGCATGGTG-3', digested (Asp718, ClaI and EcoRI, BamHI respectively) and ligated into B3D (46). All constructs were sequenced to confirm MIF sequence identity.

Protein purification and refolding. *Pf* and *Pb*MIF were expressed in BL21 (DE3) pLysS bacteria grown on Luria Broth (LB, Q-biogene) containing 30 μg/ml chloramphenicol and 0.05 μg/ml ampicillin. Bacteria were grown at 37°C to an OD600 of 0.4 and induced by the addition of isopropyl-D-thiogalactoside to a final concentration of 1 mM. After 3 hours, the cells were harvested and lysed in 50 mM TRIS (pH 8.0), 500 mM NaCl, 10% (vol/vol) glycerol, 0.01% Nonidet P-40, 10 mM β-mercaptoethanol in the presence of complete protease inhibitor cocktail (Roche) and 1 μg/ml lysozyme. Genomic DNA was fragmented by sonication, after which the lysate was cleared by centrifugation at 30,000 x g for 45 min at 4°C and loaded onto an Ni-NTA column (Qiagen) equilibrated in 50 mM TRIS (pH 8.0), 200 mM NaCl, 10% (vol/vol) glycerol, 20 mM imidazole and 10 mM β-mercaptoethanol. After washing, the protein was eluted in a linear gradient from 20–400 mM imidazole. Peak fractions were pooled, concentrated to 10 ml in an Amicon stirred ultrafiltration cell (Millipore) using a 10 kD cut-off filter and loaded on a Superdex 75 gel filtration column (Amersham Pharmacia) equilibrated in 50 mM Tris pH 8.0, 200 mM NaCl, 5% (vol/vol) glycerol and 5 mM β-mercaptoethanol. These preparations and MIF preparations of refolded lyophilised recombinant MIF (3) were confirmed to be free of LPS (<5 ng of LPS/mg of protein) by Limulus amoebocyte assay (Biowhittaker Inc., Walkersville, MD).

Oxidoreductase and tautomerase assay. Oxidoreductase and tautomerase assays were performed as described (28,43), except that ^{1}H NMR spectra during tautomerase analysis were recorded with 1-minute intervals using a Bruker DPX-300 with 3-(trimethylsilyl) tetradeuteropropionic acid sodium salt as internal standard.

Antibody generation and Western blotting. Polyclonal antibodies against *Pb*MIF were raised in New Zealand white rabbits by injecting 100 µg LPS-free *Pb*MIF linked to keyhole limpet hemocyanin (KLH) in complete Freund's adjuvant. After three boosts of 100 µg KLH –linked *Pb*MIF in incomplete Freund's adjuvant, 5 ml of serum was collected and used in 1/1000 dilution as primary antibody in Western blotting.

Immune fluorescence assays. Blood stages from overnight schizont cultures were fixed with paraformaldehyde and the c-myc tag visualized by incubation with anti c-myc monoclonal (C3956, Sigma–Aldrich, The Netherlands) followed by staining with FITC-labeled goat anti-rabbit IgG antibody. Parasite nuclei were stained using DAPI (Sigma–Aldrich, The Netherlands) using the manufacturers instructions. Fluorescence was visualized using fluorescence MDR microscopy (Leica; GFP and DAPI filter settings) and images recorded using a DC500 digital camera.

AP-1 activation assay. The AP-1 assay was used as described (25,27). Briefly, $1.7 \cdot 10^5$ HEK cells per well were plated out in 24-well cell culture plates. After 24 hours, 50 ng pAP-1-luciferase reporter plasmid and 1 ng pRenilla control plasmid (Dual-Luciferase® Reporter Assay System, Promega, Leiden, The Netherlands) were transfected per $1.7 \cdot 10^5$ HEK cells using lipofectamine 2000 (Invitrogen) as a transfection reagent. Cells were allowed to recover from transfection for 18 hours. Then, transfected cells were pre-incubated with recombinant human MIF or *P*MIF or control buffer for one hour, followed by an eight hour co-incubation with 3 nM phorbol myristate 13-acetate (PMA). Both PMA concentration and incubation time have been optimized in pilot experiments to yield the largest induction of the AP-1 promoter without causing significant cell death. Control cells (basal) were not incubated with PMA. Cells were washed and cell lysates were prepared using 100 µl passive lysis buffer (Dual-Luciferase® Reporter Assay

System, Promega) to quantify luciferase and renilla activities according to the protocol of the manufacturer.

Gene knockout and tagging in P.berghei. Transfection and selection of *pbmif*-deleted or tagged parasites was performed as previously described (29). Genomic integration of knockout and tagging vector DNA was confirmed by southern blotting of pulse-field gel electrophoresis (PFGE) separated chromosomes of the knockout or tagged parasites and probing with the 3'UTR of the PbDHFR gene. In addition, correct replacement of the *Pb*MIF locus was verified by southern blotting of AccI and AccI/XbaI digested wild type and *pbmif*-ko parasite genomic DNA and probing with the upstream (-1200 to -300) *pbmif* knockout target region. The *pbmif*-ko lines and the line expressing c-myc tagged *Pb*MIF were cloned using limiting dilution, whereas the line expressing GFP tagged *Pb*MIF was not.

Virulence experiments. In two experiments, five hosts (mouse strains BALB/c and C57BL/6) were infected with HP-ANKA wild type *Plasmodium berghei* parasites and five with *pbmif*-ko parasites (*pbmif*-ko1). In addition in the second experiment, five hosts for both mouse strains were also infected with a second independently generated *pbmif*-ko parasite line (*pbmif*-ko2). All parasite lines were generated from the same stock (passage number). All mice (Haarlan, UK) were randomised into groups with respect to weight and red blood cell count and IP infected with 1×10^5 ring-stage parasites and monitored daily from day three post infection (PI). Every day of sampling, mice were weighed, thin smears made and their red blood cell densities calculated from flow-cytometry (the number of mature red blood cells and reticulocytes in the size range 3.3–10μm in diameter in 2μl of tail blood were counted according to the manufacturer's instructions; Coulter Electronics, UK). Mice were sampled until parasitaemias became very high (>50%) and/or substantial mortality occurred: day 12PI in BALB/c hosts and day 7PI in C57BL/6 hosts.

153 *Analysis of virulence experiments.* The proportion of parasitized red cells (parasitaemia) and
154 proportion of red cells that were reticulocytes (reticulocytaemia) were calculated daily from thin
155 smears and transformed to parasite and reticulocyte densities using red cell density counts. The
156 following summary statistics for each infected host were calculated: cumulative densities for
157 parasites and reticulocytes; red cell and mass loss; minimum red cell density and mass; peak
158 parasitaemia and reticulocytaemia. Proportion data were arcsin-squareroot transformed to
159 comply with the assumptions of parametric tests. For all experiments, general linear models
160 (GLM; R Foundation for Statistical Computing, Austria) were used to compare infection
161 parameters between *pbmif*-ko and wild type infections and Tukey tests used to determine which
162 groups differed when significant results were obtained.

Results

MIF is expressed constitutively by Plasmodium and secreted by blood stage forms

MIF homologues have previously been described in a number of parasitic nematodes (20,48,49) and have now also been found in *Apicomplexans*, including *Plasmodium* (PlasmoDB entry *Pf*MIF: PFL1420w; GeneDB entry *Pb*MIF: PB000372.03.0). These parasite MIFs share moderate homology with mammalian MIF and with each other (29% identity and 39% similarity between huMIF and *Pf*MIF; figure 1A). Nevertheless crystal structure determination of nematode MIF protein revealed that the overall structure of these diverged MIF proteins is highly conserved (45) and thus the sequence of parasite MIFs can be accurately threaded onto the human MIF structure. Conserved residues, shown in ball-and-stick in the crystal structure of huMIF (33), mainly cluster around the tautomerase active site (residues 2, 32-34, 64-66; Figure 1B) indicating that the tautomerase activity is likely to be a shared property between mammalian and parasitic MIFs. In contrast, the second cysteine in the mammalian MIF CXXC oxidoreductase motif does not seem to be as well conserved throughout the parasitic MIFs (boxed region in figure 1A).

To determine the expression profile of *Pb*MIF, we analyzed various stages of *P.berghei* infection by Northern blotting. *Pbmif* is transcribed throughout the asexual blood stages, with peak steady-state mRNA levels observed at the late trophozoite and early schizont stages (figure 2A). Furthermore, we tracked *Pb*MIF protein expression by the generation of a knock-in *P.berghei* strain expressing C-terminal GFP-tagged *Pb*MIF under control of the endogenous promoter (figure 7B). Since the GFP-tag is about three times the molecular weight of the *Pb*MIF monomer, its presence may affect the cellular distribution of *Pb*MIF. Therefore, we do not draw any conclusion with regards to cellular localization of the fusion, other than presence or absence

186 at the given stage of the life cycle. *Pb*MIF-GFP was found to be expressed ubiquitously in the
187 blood stages and in mosquito-stage ookinetes and sporozoites (figure 2B-I).

188 Any function of *P*MIF in parasite-host interaction or immune evasion would require
189 *P*MIF to be externalised by the parasite. However, like mammalian MIF, which is exported by
190 non-classical pathways likely involving an ABCA1 transporter (21), *P*MIF has no signal
191 sequence. To analyse whether *P*MIF is released from parasite-infected erythrocytes, we
192 developed a polyclonal antibody specific for *Pb*MIF and immuno-blotted supernatants and
193 lysates of synchronous, cultured *P.berghei* blood stage parasites. This antibody showed
194 extremely low cross reactivity with recombinant huMIF on a long exposure (> 5 min.) of the blot
195 (figure 3A, lanes 12-13), which is virtually identical to murine MIF (muMIF; 89% identity, 95%
196 homology). Nevertheless, to prevent any confounding presence of muMIF, we removed all
197 leucocytes by passing the sample over a Plasmodipur filter (Euro-Diagnostica, Arnhem, The
198 Netherlands). When grown in culture, *P.berghei* blood stage parasites arrest in the late schizont
199 stage, since the infected erythrocytes fail to rupture (47). This allows a discrimination to be made
200 between active secretion throughout asexual growth and release by the infected erythrocyte at the
201 time of schizont rupture. Figure 3A shows that significant levels of *Pb*MIF are present in the
202 cytoplasm of the infected erythrocyte in both trophozoite and schizont stages. A small quantity
203 of *Pb*MIF was also detected in the culture supernatant but the amount varied between
204 experiments (not shown) and so was likely released by mechanical shearing of infected
205 erythrocytes. Mechanical rupture of the parasitophorous vacuole of the schizonts, releasing the
206 merozoites, resulted in the release of an additional burst of *Pb*MIF. Lysis of trophozoites or
207 merozoites released additional MIF.

208 Rabbit polyclonal *Pb*MIF antisera showed high non-specific cross-reactivity in
209 immunofluorescence assay, precluding direct visualisation of *Pb*MIF in infected cells. Therefore,

a knock-in *P.berghei* strain expressing *Pb*MIF with the much smaller (2.7 kD) C-terminal c-myc tag (figure 7B) was generated, enabling direct detection of the fusion using monoclonal anti-c-myc antibodies. Figure 3B-1 shows staining of the parasitophorous vacuole in trophozoites and schizonts, along with a faint staining of the infected erythrocyte cytoplasm in the trophozoite. Schizont rupture resulted in a loss of fluorescence (figure 3B-2), consistent with the results in the figure 3A.

Expression and purification of recombinant PMIF-his$_6$ and measurement of enzymatic activities

Although all MIFs are structurally conserved, the conservation of the residues associated with the two known enzymatic activities is greater for the tautomerase activity than those of the oxidoreductase activity. Since the N-terminal proline is the catalytic residue in the tautomerase activity (33) and we wished to compare the enzymatic properties of *P*MIF with huMIF, we generated chose to locate the His$_6$ tag at the C-terminus well away from any enzymatic site in our *Pb*, *Pf* and huMIF expression constructs. The major peak of *P*MIF-his$_6$ elutes at an apparent size of 30 kD on a size exclusion column, while huMIF-his$_6$ elutes at an apparent size of 22 kD. Both values are consistent with a dimeric form in solution (figure 4A). We tested tautomerase activity of the purified recombinant *P*MIF-his$_6$ by monitoring the conversion of p-hydroxyphenylpyruvate from the enol to the keto form by ^{1}H-NMR (43). *Pf* and *Pb*MIF-his$_6$ showed appreciable tautomerase activity above the background level of the mock purification control, but with a five-fold lower activity than huMIF-his$_6$ wild type, which served as control (figure 4B). We next tested whether *P*MIF-his$_6$ exerts oxidoreductase activity and quantified the NADPH-dependent reduction of 2-hydroxyethyldisulfide (HED). Figure 4C shows that the oxidoreductase activity of *Pf*MIF-his$_6$ is able to catalyse the reduction of HED at levels above the mock purification control. Surprisingly, given the lack of conservation, the oxidoreductase activity is also only reduced about five-fold compared to the huMIF-his$_6$ wild type control. In

234 both assays, *Pb*MIF-his$_6$ showed less activity than *Pf*MIF-his$_6$. Given the high level of
235 conservation between these two MIFs, however, this is unlikely to be a lower intrinsic activity,
236 but rather may reflect small differences in refolding efficiency.
237 *Recombinant PMIF is equally efficient as huMIF in inhibiting AP-1 stimulation*
238 We investigated if the *in vivo* activity of *P*MIF-his$_6$ would mirror the reduced enzymatic activity
239 of *P*MIF-his$_6$ compared to huMIF-his$_6$. HuMIF can reduce AP-1 expression by physically
240 interacting with transcriptional coactivator Jab-1; an activity at least partially dependent upon the
241 oxidoreductase activity of huMIF (27). Therefore, we used an AP-1 reporter assay in human
242 embryonic kidney cells (HEK) to examine the biological activity of recombinant *P*MIF-his$_6$.
243 Figure 5 shows that, although both huMIF-his$_6$ and *P*MIF-his$_6$ both showed a trend towards
244 repression of basal expression of AP-1, this effect became statistically relevant ($p<0.05$ at $n\geq6$)
245 only after AP-1 expression was induced with phorbol myristate 13-acetate (PMA). The induction
246 of the AP-1 promoter by MPA was quite subtle in HEK cells. Higher levels of induction could be
247 achieved by increasing PMA concentration and incubation time, but were invariably associated
248 with increased cell death. Nevertheless, the repression effect was in the same order of magnitude
249 for both huMIF-his$_6$ and *P*MIF-his$_6$, which implies that *P*MIF is able to bind to and interfere
250 with Jab-1 to the same extent as huMIF despite its reduced oxidoreductase activity.
251 *PbMIF-knockout parasites are viable throughout the life cycle and increase host reticulocyte*
252 *density***.**
253 To investigate the role of *Pb*MIF during *in vivo* infection in the mouse host and mosquito vector,
254 two independent *pbmif*-ko parasite lines were generated using double crossover gene
255 replacement. Correct integration of the selection marker and disruption of the *pbmif* locus was
256 confirmed by pulse-field gel electrophoresis, PCR (not shown) and Southern blotting (figure 7).
257 *Pbmif*-ko parasites are viable *in vivo*, replicate asexually at the same rate as wild type parasites,

form sexual-stage parasites at the wild-type frequency and transmit throughout the full life cycle (not shown). Since *Pb*MIF may have a more subtle role in parasite-host interactions, we investigated *pbmif*-ko parasite virulence and infection dynamics in two in-bred mouse strains: BALB/c and C57BL/6.

In C57BL/6 mice, *P. berghei* ANKA infection (IP injection of 1 x 10^5 parasites) generally leads to cerebral complications, presenting as ataxia, shivering, lethargy and death at days 8-9 of infection as parasitaemia reaches ~10% (16,19). *P. berghei* ANKA infection in BALB/c mice may lead to similar cerebral complications in a small proportion of mice or, more commonly, a syndrome termed severe malaria (18,19) in which mice suffer severe anaemia, weight loss and organ damage from day 8 of infection associated with a high parasitaemia. Mice infected with wild type or *pbmif*-ko parasites showed symptoms consistent with these syndromes; infection in C57Bl/6 mice resulted in death at day 8PI and infection in BALB/c mice resulted in high parasitaemia and severe anaemia (tables 1 and 2) in all cases.

In both experiments, with two independently-generated *pbmif*-ko lines and two mouse strains, hosts infected with *pbmif*-ko lines had significantly higher reticulocyte densities and peak reticulocytaemias than those infected with wild type parasites (figure 6; tables 1 and 2). In contrast, none of the other virulence parameters revealed consistently significant differences between infections with *pbmif*-ko and wild type parasites. In both experiments, infections with the first *pbmif*-ko line (*pbmif*-ko1) did not differ significantly from infections with wild type parasites in: cumulative parasite density; peak parasitaemia; minimum mass; mass loss; minimum red cell density or red cell loss. When comparing infections initiated with the second *pbmif*-ko line (*pbmif*-ko2) to infections with wild type parasites, there were no significant differences in: peak parasitaemia; minimum mass; mass loss or red cell loss. However, when compared to infections with wild type parasites, *pbmif*-ko2 parasites had significantly higher

cumulative parasite densities, but only in BALB/c mice, and reached significantly lower minimum red cell densities, but only in C57BL/6 mice. Therefore, only reticulocyte parameters differed consistently and significantly between both *pbmif*-ko lines and wild type infections in BALB/c and C57BL/6 mice (figure 6; tables 1 & 2).

Discussion

It is now clear that the cytokine MIF is an evolutionary ancient protein with a widespread distribution. MIF homologues have been functionally characterized in parasitic nematodes (20,49). Furthermore, genome-sequencing projects show that MIF homologues are present in the protozoan parasites *Toxoplasma gondii* and *Leishmania major* but absent from the published genomes of other protozoans including the related *Apicomplexan* parasites, *Cryptosporidium parvum, Theileria parvum* and *T. Annulata* and free-living eukaryotes, including *Dictyostelium discoidium* and the ciliate, *Tetrahymena thermophila*. Thus, at present the expression of MIF homologues in unicellular eukaryotes is consistently associated with a group of parasitic protozoa that engage in specialised interactions with host cells in blood. Here we describe an initial functional characterization of the *Plasmodium* MIF homologue. Of note, the use of the term "homologue" instead of "orthologue" in the case of parasite derived MIF is justified, since while we show conservation in function, we cannot at this time rule out additional properties of parasite derived MIF that are not shared with host MIF.

While *Pb*MIF transcription appears to peak at the trophozoite stage in asexual blood stage parasites, *Pb*MIF is expressed in all parasite forms examined throughout the life cycle and distributed in the cytoplasm of both the parasite and the infected erythrocyte. These results correlate with *P. falciparum* transcriptome data (5,31) (PlasmoDB entry PFL1420w). Furthermore, proteome surveys indicate that the protein is also present in all *P. falciparum* and

306 *P. berghei* life cycle stages analysed (22,24). The apparent discrepancy between messenger and
307 protein presence might be explained by differences in protein and mRNA stability and turnover.
308 In blood stage parasites, release of *P*MIF is most likely episodic coinciding with rupture of the
309 infected erythrocyte and the release of merozoites. Recombinant his_6 tagged *P*MIF and huMIF
310 elute with apparent molecular weights of 30 and 22 kD in size exclusion chromatography, both
311 consistent with a dimeric form in solution. Until recently, the oligomerization state of huMIF had
312 been under debate, with reports showing monomeric, dimeric and trimeric forms based on
313 crosslinking experiments and dimeric forms in size exclusion chromatography. A trimeric form
314 in solution was firmly established in sedimentation equilibrium studies (40) (and references
315 therein). Since *P*MIF-his_6 appear to behave in a similar way as huMIF-his_6 on size exclusion
316 chromatography and huMIF-his_6 appears to behave as untagged huMIF in previous work (37),
317 the his_6 tag does not appear to affect oligomerization. However, a more in depth study would be
318 required to determine the exact oligomerization status of *P*MIF in solution.
319 There have been conflicting reports about the relevance of the C-terminus of huMIF with
320 regards to enzymatic activity (2,36). In our assays, a C-terminal his_6 tag did not appear to
321 influence enzymatic activity. Recombinant *P*MIF-his_6 show tautomerase and oxidoreductase
322 activity, although in both assays the activities are ~20% of recombinant huMIF-his_6. It is
323 surprising that *P*MIF-his_6 retains oxidoreductase activity in the absence of the second cysteine of
324 the CXXC motif and low conservation of surrounding sequences. However, given this low
325 conservation, we cannot directly compare the *P*MIF and its oxidoreductase activity to the human
326 C60S MIF mutant (which retained only background activity compared to wtMIF in the HED
327 assay). For example, the cysteine in *P*MIF that would correspond to C57 in mammalian MIF is
328 shifted by one register in the alignment (figure 1A). Rather, the remaining oxidoreductase
329 activity in *P*MIF can be seen as an intermediate form between the human C57S MIF (which

retains about 60% of wtMIF activity in the HED assay) and C60S MIF (28). However, we cannot exclude that the N-terminal cysteine residues may contribute to this effect by transferring protons from reduced glutathione to HED. It is also possible that the structural requirements for oxidoreductase activity are fulfilled in the *P*MIF multimer.

Despite this relatively low enzymatic activity and low sequence similarity compared to huMIF, we have shown that recombinant *P*MIF-his$_6$ and the huMIF-his$_6$ control are equally efficient in reducing AP-1 activation in HEK cells. The exact structural requirements for Jab-1 binding and the inhibition of Jab-1 mediated activation of AP-1 are currently unknown. Previous studies imply that in huMIF, a structural rearrangement involving the oxidoreductase activity (involving C60) is required for this activity (8,27,38). However, peptides spanning the CXXC motif with either wild type or C57S/C60S double point mutant sequence can both compete for huMIF binding to Jab-1(27). In the absence of a strong oxidoreductase activity and the crucial C60 in *P*MIF, therefore, structural differences may account for *P*MIF's ability to inhibit Jab-1 function. Alternatively, differences in protein uptake or stability in HEK cells between *P*MIF and huMIF might explain this effect.

*P*MIF is not essential for any phase of the *Plasmodium* life cycle. Furthermore deletion of *Pb*MIF did not consistently influence standard virulence parameters, such as red blood cell loss, weight loss and parasite growth, in the early stages of a *P. berghei* infection. However, infections in two host strains revealed a clear and significant increase in reticulocyte production in the early stages of *pbmif*-ko infection such that *pbmif*-ko infected hosts have 1.5-4.5 fold more circulating reticulocytes than wild type infected hosts. Accurately characterizing the phenotypic effects of MIF expression is difficult using these combinations of *P. berghei* and inbred mice due to the rapid and lethal progression of infections. Such studies may be more informative if carried out in *P. chabaudi*, which causes a chronic infection in inbred mouse strains. These studies will rely on

354 the *P. chabaudi* genetic transformation technology that has been developed recently (Reece and
355 Thompson, in preparation).

356 None of the studies on host MIF response to *Plasmodium* infection published thus far
357 have taken the presence of parasite encoded MIF into account (1,13,14,15,34,35). Intriguingly,
358 two of these studies clearly show a role for MIF as a host-derived factor inhibiting erythropoiesis
359 in the context of *P. chabaudi* infection in BALB/c mice (34,35). Our results showing increased
360 reticulocyte numbers in *pbmif*-ko infections match well with these studies and indicate that
361 parasite-encoded MIF might work in concert with host MIF to suppress erythropoiesis in the
362 context of a *Plasmodium* infection. Furthermore, McDevitt *et al* found a mild increase in host
363 survival when the infection was carried out in MIF knockout mice. Therefore it will be of
364 interest to follow the course of infection of the *pbmif*-ko parasite in a MIF knockout mouse
365 strain. At this moment it is unclear how this inhibitory effect on reticulocyte numbers might
366 benefit the parasite; since *P. berghei* is a reticulocyte-preferring parasite, *Pb*MIF appears to be
367 acting to reduce the preferred host blood cell pool for invasion. However, suppression of
368 erythropoiesis may lead to maintenance of a lower parasitaemia, which might contribute to a
369 longer lasting infection. Thus it is clear that further research on the behaviour of the *pmif*-ko
370 parasites in the context of chronic and also genetically diverse infections, is required to
371 understand the action of *P*MIF.

372 Since MIF is a central regulator of the inflammatory response in vertebrates (reviewed in
373 (11)), release of a parasite homologue is likely to influence this response. It would seem counter-
374 intuitive that parasites would produce a protein that could both initiate a potentially lethal
375 inflammatory immune response and demonstrably reduce the population of red cells preferred
376 for asexual proliferation. However, huMIF has been shown to be able to act upon both pro- and
377 anti-inflammatory pathways, depending on context and concentration (27), reviewed in (11).

This raises the intriguing possibility that parasites produce MIF homologues to subversively switch the host immune response from a pro- to anti-inflammatory setting, for instance by expressing an excess amount of parasite MIF that competes with host MIF for effector binding sites and so desensitises host signalling for the pro-inflammatory response. Preliminary data indeed shows that *P*MIF binds to CD74, which has been identified as a MIF surface receptor (32), with higher affinity than huMIF (unpublished observation). We are currently generating a transgenic *P.berghei* parasite, which over-expresses *Pb*MIF in the hope that further characterization of the role of *P*MIF in an in vivo setting and further biochemical studies with recombinant *P*MIF will provide additional insights into the role of this cytokine homologue in relation to host response. Alternatively, parasites may be purposefully inducing an inflammatory response, using the host immune system as a means to regulate the population of competing parasites within hosts. Further characterization of host responses to *P*MIF after short term as well as long-term exposure will be required to distinguish between these two possibilities. Finally since parasite MIF homologues are not limited to *Plasmodium*, the findings presented in this study will have implications for the study of host-parasite dynamics in other parasites.

Acknowledgements

We wish to thank Jai Ramesar for technical assistance with the *P.berghei* transfections and Professors Andrew Read, Rick Maizels and Judith Allen for critical reading of the manuscript and useful discussions. This work was supported by The Wellcome Trust grant number 072171 and The Netherlands Organization for Scientific Research grant numbers 812.05.002 and 816.02.001.

Reference list

1. **Awandare, G. A., Hittner, J. B., Kremsner, P. G., Ochiel, D. O., Keller, C. C., Weinberg, J. B., Clark, I. A., and Perkins, D. J.** (2006). Decreased circulating macrophage migration inhibitory factor (MIF) protein and blood mononuclear cell MIF transcripts in children with Plasmodium falciparum malaria. Clin.Immunol. **119**: 219-225.

2. **Bendrat, K., Al Abed, Y., Callaway, D. J., Peng, T., Calandra, T., Metz, C. N., and Bucala, R.** (1997). Biochemical and mutational investigations of the enzymatic activity of macrophage migration inhibitory factor. Biochemistry **36**: 15356-15362.

3. **Bernhagen, J., Mitchell, R. A., Calandra, T., Voelter, W., Cerami, A., and Bucala, R.** (1994). Purification, bioactivity, and secondary structure analysis of mouse and human macrophage migration inhibitory factor (MIF). Biochemistry **33**: 14144-14155.

4. **Bloom, B. R. and Bennett, B.** (1966). Mechanism of a reaction in vitro associated with delayed-type hypersensitivity. Science **153**: 80-82.

5. **Bozdech, Z., Llinas, M., Pulliam, B. L., Wong, E. D., Zhu, J., and DeRisi, J. L.** (2003). The Transcriptome of the Intraerythrocytic Developmental Cycle of Plasmodium falciparum. PLoS.Biol. **1**: E5.

6. **Bozza, M., Satoskar, A. R., Lin, G., Lu, B., Humbles, A. A., Gerard, C., and David, J. R.** (1999). Targeted disruption of migration inhibitory factor gene reveals its critical role in sepsis. J.Exp.Med. **189**: 341-346.

7. **Breman, J. G.** (2001). The ears of the hippopotamus: manifestations, determinants, and estimates of the malaria burden. Am.J.Trop.Med.Hyg. **64**: 1-11.

8. **Burger-Kentischer, A., Finkelmeier, D., Thiele, M., Schmucker, J., Geiger, G., Tovar, G. E., and Bernhagen, J.** (2005). Binding of JAB1/CSN5 to MIF is mediated by the MPN domain but is independent of the JAMM motif. FEBS Lett. **579**: 1693-1701.

9. **Calandra, T., Bernhagen, J., Metz, C. N., Spiegel, L. A., Bacher, M., Donnelly, T., Cerami, A., and Bucala, R.** (1995). MIF as a glucocorticoid-induced modulator of cytokine production. Nature **377**: 68-71.

10. **Calandra, T., Bernhagen, J., Mitchell, R. A., and Bucala, R.** (1994). The macrophage is an important and previously unrecognized source of macrophage migration inhibitory factor. J.Exp.Med. **179**: 1895-1902.

11. **Calandra, T. and Roger, T.** (2003). Macrophage migration inhibitory factor: a regulator of innate immunity. Nat.Rev.Immunol. **3**: 791-800.

12. **Calandra, T., Spiegel, L. A., Metz, C. N., and Bucala, R.** (1998). Macrophage migration inhibitory factor is a critical mediator of the activation of immune cells by exotoxins of Gram-positive bacteria. Proc.Natl.Acad.Sci.U.S.A **95**: 11383-11388.

13. **Chaisavaneeyakorn, S., Lucchi, N., Abramowsky, C., Othoro, C., Chaiyaroj, S. C., Shi, Y. P., Nahlen, B. L., Peterson, D. S., Moore, J. M., and Udhayakumar, V.** (2005). Immunohistological characterization of macrophage migration inhibitory factor expression in Plasmodium falciparum-infected placentas. Infect.Immun. **73**: 3287-3293.

14. **Chaisavaneeyakorn, S., Moore, J. M., Othoro, C., Otieno, J., Chaiyaroj, S. C., Shi, Y. P., Nahlen, B. L., Lal, A. A., and Udhayakumar, V.** (2002). Immunity to placental malaria. IV. Placental malaria is associated with up-regulation of macrophage migration inhibitory factor in intervillous blood. J.Infect.Dis. **186**: 1371-1375.

15. **Chaiyaroj, S. C., Rutta, A. S., Muenthaisong, K., Watkins, P., Na, U. M., and Looareesuwan, S.** (2004). Reduced levels of transforming growth factor-beta1, interleukin-12 and increased migration inhibitory factor are associated with severe malaria. Acta Trop. **89**: 319-327.

16. **Curfs, J. H., Hermsen, C. C., Kremsner, P., Neifer, S., Meuwissen, J. H., Van Rooyen, N., and Eling, W. M.** (1993). Tumour necrosis factor-alpha and macrophages in Plasmodium berghei-induced cerebral malaria. Parasitology **107 (Pt 2)**: 125-134.

17. **David, J. R.** (1966). Delayed hypersensitivity in vitro: its mediation by cell-free substances formed by lymphoid cell-antigen interaction. Proc.Natl.Acad.Sci.U.S.A **56**: 72-77.

18. **de Kossodo, S. and Grau, G. E.** (1993). Profiles of cytokine production in relation with susceptibility to cerebral malaria. J.Immunol. **151**: 4811-4820.

19. **Delahaye, N. F., Coltel, N., Puthier, D., Flori, L., Houlgatte, R., Iraqi, F. A., Nguyen, C., Grau, G. E., and Rihet, P.** (2006). Gene-Expression Profiling Discriminates between Cerebral Malaria (CM)-Susceptible Mice and CM-Resistant Mice. J.Infect.Dis. **193**: 312-321.

20. **Falcone, F. H., Loke, P., Zang, X., MacDonald, A. S., Maizels, R. M., and Allen, J. E.** (2001). A Brugia malayi homolog of macrophage migration inhibitory factor reveals an important link between macrophages and eosinophil recruitment during nematode infection. J.Immunol. **167**: 5348-5354.

21. **Flieger, O., Engling, A., Bucala, R., Lue, H., Nickel, W., and Bernhagen, J.** (2003). Regulated secretion of macrophage migration inhibitory factor is mediated by a non-classical pathway involving an ABC transporter. FEBS Lett. **551**: 78-86.

22. **Florens, L., Washburn, M. P., Raine, J. D., Anthony, R. M., Grainger, M., Haynes, J. D., Moch, J. K., Muster, N., Sacci, J. B., Tabb, D. L., Witney, A. A., Wolters, D., Wu, Y., Gardner, M. J., Holder, A. A., Sinden, R. E., Yates, J. R., and Carucci, D. J.** (2002). A proteomic view of the Plasmodium falciparum life cycle. Nature **419**: 520-526.

23. **Gardner, M. J., Hall, N., Fung, E., White, O., Berriman, M., Hyman, R. W., Carlton, J. M., Pain, A., Nelson, K. E., Bowman, S., Paulsen, I. T., James, K., Eisen, J. A., Rutherford, K., Salzberg, S. L., Craig, A., Kyes, S., Chan, M. S., Nene, V., Shallom, S. J., Suh, B., Peterson, J., Angiuoli, S., Pertea, M., Allen, J., Selengut, J., Haft, D., Mather, M. W., Vaidya, A. B., Martin, D. M., Fairlamb, A. H., Fraunholz, M. J., Roos, D. S., Ralph, S. A., McFadden, G. I., Cummings, L. M., Subramanian, G. M., Mungall, C., Venter, J. C., Carucci, D. J., Hoffman, S. L., Newbold, C., Davis, R. W., Fraser, C. M., and Barrell, B.** (2002). Genome sequence of the human malaria parasite Plasmodium falciparum. Nature **419**: 498-511.

24. **Hall, N., Karras, M., Raine, J. D., Carlton, J. M., Kooij, T. W., Berriman, M., Florens, L., Janssen, C. S., Pain, A., Christophides, G. K., James, K., Rutherford, K., Harris, B., Harris, D., Churcher, C., Quail, M. A., Ormond, D., Doggett, J., Trueman, H. E., Mendoza, J., Bidwell, S. L., Rajandream, M. A., Carucci, D. J., Yates, J. R., III, Kafatos, F. C., Janse, C. J., Barrell, B., Turner, C. M., Waters, A. P., and Sinden, R. E.** (2005). A comprehensive survey of the Plasmodium life cycle by genomic, transcriptomic, and proteomic analyses. Science **307**: 82-86.

25. **Haslinger, B., Kleemann, R., Toet, K. H., and Kooistra, T.** (2003). Simvastatin suppresses tissue factor expression and increases fibrinolytic activity in tumor necrosis factor-alpha-activated human peritoneal mesothelial cells. Kidney Int. **63**: 2065-2074.

26. **Hoerauf, A., Satoguina, J., Saeftel, M., and Specht, S.** (2005). Immunomodulation by filarial nematodes. Parasite Immunol. **27**: 417-429.

27. **Kleemann, R., Hausser, A., Geiger, G., Mischke, R., Burger-Kentischer, A., Flieger, O., Johannes, F. J., Roger, T., Calandra, T., Kapurniotu, A., Grell, M., Finkelmeier, D., Brunner, H., and Bernhagen, J.** (2000). Intracellular action of the cytokine MIF to modulate AP-1 activity and the cell cycle through Jab1. Nature **408**: 211-216.

28. **Kleemann, R., Kapurniotu, A., Frank, R. W., Gessner, A., Mischke, R., Flieger, O., Juttner, S., Brunner, H., and Bernhagen, J.** (1998). Disulfide analysis reveals a role for macrophage migration inhibitory factor (MIF) as thiol-protein oxidoreductase. J.Mol.Biol. **280**: 85-102.

29. **Koning-Ward, T. F., Janse, C. J., and Waters, A. P.** (2000). The development of genetic tools for dissecting the biology of malaria parasites. Annu.Rev.Microbiol. **54**: 157-185.

30. **Kooij, T. W., Franke-Fayard, B., Renz, J., Kroeze, H., van Dooren, M. W., Ramesar, J., Augustijn, K. D., Janse, C. J., and Waters, A. P.** (2005). Plasmodium berghei alpha-tubulin II: a role in both male gamete formation and asexual blood stages. Mol.Biochem.Parasitol. **144**: 16-26.

31. **Le Roch, K. G., Zhou, Y., Blair, P. L., Grainger, M., Moch, J. K., Haynes, J. D., De, L., V, Holder, A. A., Batalov, S., Carucci, D. J., and Winzeler, E. A.** (2003). Discovery of gene function by expression profiling of the malaria parasite life cycle. Science **301**: 1503-1508.

32. **Leng, L., Metz, C. N., Fang, Y., Xu, J., Donnelly, S., Baugh, J., Delohery, T., Chen, Y., Mitchell, R. A., and Bucala, R.** (2003). MIF signal transduction initiated by binding to CD74. J.Exp.Med. **197**: 1467-1476.

33. **Lubetsky, J. B., Swope, M., Dealwis, C., Blake, P., and Lolis, E.** (1999). Pro-1 of macrophage migration inhibitory factor functions as a catalytic base in the phenylpyruvate tautomerase activity. Biochemistry **38**: 7346-7354.

34. **Martiney, J. A., Sherry, B., Metz, C. N., Espinoza, M., Ferrer, A. S., Calandra, T., Broxmeyer, H. E., and Bucala, R.** (2000). Macrophage migration inhibitory factor release by macrophages after ingestion of Plasmodium chabaudi-infected erythrocytes: possible role in the pathogenesis of malarial anemia. Infect.Immun. **68**: 2259-2267.

35. **McDevitt, M. A., Xie, J., Shanmugasundaram, G., Griffith, J., Liu, A., McDonald, C., Thuma, P., Gordeuk, V. R., Metz, C. N., Mitchell, R., Keefer, J., David, J., Leng, L., and Bucala, R.** (2006). A critical role for the host mediator macrophage migration inhibitory factor in the pathogenesis of malarial anemia. J.Exp.Med.

36. **Mischke, R., Gessner, A., Kapurniotu, A., Juttner, S., Kleemann, R., Brunner, H., and Bernhagen, J.** (1997). Structure activity studies of the cytokine macrophage migration inhibitory factor (MIF) reveal a critical role for its carboxy terminus. FEBS Lett. **414**: 226-232.

37. **Mischke, R., Kleemann, R., Brunner, H., and Bernhagen, J.** (1998). Cross-linking and mutational analysis of the oligomerization state of the cytokine macrophage migration inhibitory factor (MIF). FEBS Lett. **427**: 85-90.

38. **Nguyen, M. T., Beck, J., Lue, H., Funfzig, H., Kleemann, R., Koolwijk, P., Kapurniotu, A., and Bernhagen, J.** (2003). A 16-residue peptide fragment of macrophage migration inhibitory factor, MIF-(50-65), exhibits redox activity and has MIF-like biological functions. J.Biol.Chem. **278**: 33654-33671.

39. **Pastrana, D. V., Raghavan, N., FitzGerald, P., Eisinger, S. W., Metz, C., Bucala, R., Schleimer, R. P., Bickel, C., and Scott, A. L.** (1998). Filarial nematode parasites secrete a homologue of the human cytokine macrophage migration inhibitory factor. Infect.Immun. **66**: 5955-5963.

40. **Philo, J. S., Yang, T. H., and LaBarre, M.** (2004). Re-examining the oligomerization state of macrophage migration inhibitory factor (MIF) in solution. Biophys.Chem. **108**: 77-87.

41. **Reininger, L., Billker, O., Tewari, R., Mukhopadhyay, A., Fennell, C., Dorin-Semblat, D., Doerig, C., Goldring, D., Harmse, L., Ranford-Cartwright, L., Packer, J., and Doerig, C.** (2005). A NIMA-related protein kinase is essential for completion of the sexual cycle of malaria parasites. J.Biol.Chem. **280**: 31957-31964.

42. **Rodriguez-Sosa, M., Rosas, L. E., David, J. R., Bojalil, R., Satoskar, A. R., and Terrazas, L. I.** (2003). Macrophage migration inhibitory factor plays a critical role in mediating protection against the helminth parasite Taenia crassiceps. Infect.Immun. **71**: 1247-1254.

43. **Rosengren, E., Bucala, R., Aman, P., Jacobsson, L., Odh, G., Metz, C. N., and Rorsman, H.** (1996). The immunoregulatory mediator macrophage migration inhibitory factor (MIF) catalyzes a tautomerization reaction. Mol.Med. **2**: 143-149.

44. **Satoskar, A. R., Bozza, M., Rodriguez, S. M., Lin, G., and David, J. R.** (2001). Migration-inhibitory factor gene-deficient mice are susceptible to cutaneous Leishmania major infection. Infect.Immun. **69**: 906-911.

45. **Swope, M., Sun, H. W., Blake, P. R., and Lolis, E.** (1998). Direct link between cytokine activity and a catalytic site for macrophage migration inhibitory factor. EMBO J. **17**: 3534-3541.

46. **van Dijk, M. R., Janse, C. J., Thompson, J., Waters, A. P., Braks, J. A., Dodemont, H. J., Stunnenberg, H. G., van Gemert, G. J., Sauerwein, R. W., and Eling, W.** (2001). A central role for P48/45 in malaria parasite male gamete fertility. Cell **104**: 153-164.

47. **Waters, A. P., Thomas, A. W., van Dijk, M. R., and Janse, C. J.** (1997). Transfection of malaria parasites. Methods **13**: 134-147.

48. **Wu, Z., Boonmars, T., Nagano, I., Nakada, T., and Takahashi, Y.** (2003). Molecular expression and characterization of a homologue of host cytokine macrophage migration inhibitory factor from Trichinella spp. J.Parasitol. **89**: 507-515.

49. **Zang, X., Taylor, P., Wang, J. M., Meyer, D. J., Scott, A. L., Walkinshaw, M. D., and Maizels, R. M.** (2002). Homologues of human macrophage migration inhibitory factor from a parasitic nematode. Gene cloning, protein activity, and crystal structure. J.Biol.Chem. **277**: 44261-44267.

Figure legends

Figure 1. **Sequence alignments between mammalian and parasite MIFs.**

A) Sequence alignments between human, mouse, *P. berghei*, *P. falciparum* and the two *B. malayi* MIF homologues (Bm-1 and –2). The arrow indicates the N-terminal catalytic proline associated with tautomerase activity and the boxed area shows the CXXC motif associated with oxidoreductase activity in the mammalian MIFs and the parasite variants. Asterisks indicate identical residues; colons and dots denote strongly and weakly similar residues respectively. B) Ribbon representation of the huMIF crystal structure (RCSB PDB entry: 1CA7 (33)). For clarity, only one monomer of the trimer is shown. Arrows indicate the positions of the tautomerase and oxidoreductase active sites. The first cysteine of the CXXC oxidoreductase motif (C57 in huMIF) that is conserved in the parasite MIFs is shown in red. Conserved residues between the various MIFs mainly cluster around the tautomerase active site and have been highlighted in ball-and-stick representation.

Figure 2. **Expression of *Pb*MIF throughout the life cycle.**

A) Time course northern analysis of the *Pb*MIF transcript in blood stages. Whole RNA extracted at various time points from a synchronous *P.berghei* blood stage infection show production of *Pb*MIF mRNA of the expected size (~0.7 kb) peaks at 17 hours post infection (HPI) (trophozoite stage). Small quantities of transcript are also present in the sexual stages (gct 1 for enriched gametocytes and gct 2 for purified gametocytes) and the ookinete (ook). An ethidium bromide stained portion of the gel showing the 28S and 18S rRNAs is included as loading control. Protein expression of the *Pb*MIF-GFP fusion was tracked by fluorescence microscopy through the life cycle showing at 100x magnification: B) late ring / early trophozoite, C) mature trophozoite, D) schizont, E) mature ookinete (some unfertilized female gametes also visible), F and G) day 18

595 oocyst at 20x and 40x magnification, H and I) salivary gland sporozoites at 40x and 100x
596 magnification. Bars, 10 μm.
597
598 Figure 3. ***Pb*MIF is externalised by *P.berghei* and is released upon schizont rupture.**
599 A) Western blot analysis using anti-*Pb*MIF rabbit polyclonal antiserum: 1) Erythrocytes infected
600 with trophozoite stage *P.berghei* were isolated by heart puncture and lysed by osmotic shock.
601 Parasite derived MIF was pulled down from the lysis supernatant (from the equivalent of 10^7
602 infected erythrocytes) using anti-*Pb*MIF bound to Protein-G sepharose (Prot-G). 2) Control
603 pulldown of the lysis supernatant using Prot-G alone. 3) Trophozoite pellet (loaded ~$2.0x10^5$
604 parasites). 4) Control pulldown of 100 ng of recombinant C-terminally His_6-tagged (C-his)
605 *Pb*MIF using Prot-G alone. 5) Control pulldown of 100 ng of recombinant C-his *Pb*MIF using
606 anti-*Pb*MIF loaded Prot-G. 6) Supernatant (sup) (10 μl of 100ml) of an overnight schizont
607 culture. 7) Supernatant (10 μl of 20 ml) of schizonts after disruption of the host erythrocyte
608 membrane. 8) PBS wash supernatant (10 μl of 1 ml) of schizont pellet from 7. 9) Supernatant (10
609 μl of 1 ml) after mechanical rupturing of the schizonts into merozoites. 10) PBS wash
610 supernatant (10 μl of 1 ml) of the merozoites from 9. 11) Solubilised merozoite pellet (loaded
611 ~$2.0x10^5$ parasites). 12) 50 ng of recombinant C-his *Pb*MIF and 13) 100 ng of recombinant
612 HuMIF.
613 B) Immunofluorescent detection of c-myc-tagged *Pb*MIF in blood stages. Thin smears from an
614 overnight schizont culture expressing *Pb*MIF-c-myc were stained using an anti-c-myc
615 monoclonal antibody. 1) An intact schizont and a trophozoite (at the arrowhead) show staining
616 within the parasitophorous vacuole. 2) An intact and a ruptured schizont. 3) Wild type *P.berghei*
617 control stained with the anti-c-myc monoclonal. The fluorescence picture in 3 was taken at 0.6
618 second exposure, while 1 and 2 used 0.3 second. Bars, 10 μm.

Figure 4. **Recombinant *P*MIF runs as a dimer in size exclusion chromatography and is active in tautomerase and oxidoreductase assays.**

A) Chromatograms of C-terminally his_6-tagged huMIF and *Pb*MIF. The retention volume of the major peak in the C-his_6 *Pb*MIF run was 192.10 ml compared to 204.87 ml for C-his6 huMIF, which leads to a calculated molecular weight of 30 kD for *Pb*MIF and 22 kD for huMIF. Reference runs included bovine albumin (66 kD; 153.93 ml), chicken ovulbamin (45 kD; 170.93 ml), bovine carbonic anhydrase (30 kD; 192.47 ml) and bovine α-lactalbumin (14.4 kD; 217.39 ml). The inlay shows a coomassie stained protein gel of the peak fractions of *Pb*MIF, identifying the void volume peak as *Pb*MIF aggregates. The same results were obtained with *Pf*MIF (data not shown).

B) Recombinant MIF tautomerase activity on p-hydroxyphenylpyruvate (R= COOH and R'= C_6H_4-OH) and C) oxidoreductase activity on 2-hydroxyethyldisulfide (R= CH_2-OH). Sample equations are given for both conversions. The activities of *Pf*MIF and *Pb*MIF are given as percentage of huMIF activity. In both sets of experiments, *Pf*MIF and *Pb*MIF activity was above the mock purification control (asterisks denote $p < 0.05$ at $n \geq 3$).

Figure 5. **Recombinant *P*MIF can inhibit AP-1 induction comparable to huMIF.**

At basal transcription, both huMIF and *P*MIF show a non-significant trend towards inhibition of AP-1 transcription in HEK cells. However, upon stimulation with phorbol myristate 13-acetate (PMA), both huMIF and *P*MIF show a statistically relevant repression compared to buffer controls (asterisks denote $p < 0.05$ at $n \geq 6$).

Figure 6. **Parasite and reticulocyte densities in *pbmif*-ko infected mice.**

643 Mean and SE asexual stage and reticulocyte density (x10^9/ml) during infections in experiment 2,
644 using: (A.1 & A.2) BALB/c and (B.1 & B.2) C57Bl/6 mice. For each host strain, 5 infections
645 were initiated with either wild type parasites (WT) or one of two independently generated *pbmif*-
646 ko lines (KO1 and KO2). In both host strains the density of circulating reticulocytes was
647 significantly lower in infections initiated with wild type parasites when compared to infections
648 initiated with *pbmif*-ko parasites (A.1 & B.1). In contrast, the density of asexual parasites did not
649 differ significantly between infections initiated with wild type parasites and *pbmif*-ko parasites
650 (A.2 & B.2).
651
652 Figure 7. **Genetic manipulation of the *pbmif* locus.**
653 A) The *pbmif*-ko was made by double crossover replacement using the 5'UTR (-1200 to -300)
654 and 3'UTR region (+785 to +1700) from the *pbmif* gene. Gene replacement with the
655 TgDHFR/TS selection marker removed the XbaI site in the 3'UTR of *Pb*MIF and introduced an
656 additional AccI site. Sizes of restriction fragments are indicated between arrows and the hatched
657 block shows the region that was used as probe in the southern analysis in C.
658 B) The *Pb*MIF-GFP and c-myc fusions were made by a single crossover knock-in (insertion)
659 event, which results in gene duplication of *pbmif* with one of the two copies GFP- or c-myc-
660 tagged, while the second copy remains wild type.
661 C) Southern blot analysis of AccI or AccI/XbaI digested genomic DNA from wild type or
662 knockout parasites. Using the 5'UTR integration target (hatched region in A) as probe, these
663 digestions should yield fragments of 2447, 2100, 2616 and 2616 base pairs respectively.
664
665 Table 1: **Comparison of virulence parameters in infections of wild type and *pbmif*-ko**
666 **parasites.**

667 Results of experiment 1 in which (A) BALB/c hosts and, (B) C57BL/6 hosts were infected with
668 either wild type or *pbmif*-ko1 parasites. Statistics are from GLMs and the F ratio represents the
669 variance attributable to each explanatory variable when compared the variance remaining
670 unexplained by the model. This ratio is weighted by the degrees of freedom associated with each
671 explanatory variable and compared to the appropriate F distribution to generate the P value. For
672 all variables, means and standard errors are presented. Variables for which wild type infections
673 differed significantly from *pbmif*-ko infections are highlighted in bold and further explanation
674 provided. Means are % for proportion data and $x10^9$/ml for density data.
675
676 Table 2: **Comparison of virulence parameters in infections of wild type and two**
677 **independently-generated *pbmif*-ko parasites.**
678 Results of experiment 2 in which in which (A) BALB/c hosts and (B) C57BL/6 hosts were
679 infected with either wild type or one of two independent lines of *pbmif*-ko parasites (*pbmif*-ko1
680 and *pbmif*-ko2). Statistics are from GLMs and the F ratio represents the variance attributable to
681 each explanatory variable when compared the variance remaining unexplained by the model.
682 This ratio is weighted by the degrees of freedom associated with each explanatory variable and
683 compared to the appropriate F distribution to generate the P value. For all variables, means and
684 standard errors are presented. Variables for which wild type infections differed significantly
685 from *pbmif*-ko infections are highlighted in bold and further explanation provided. Means are %
686 for proportion data and $x10^9$/ml for density data.

Table 1(a)

Variable	Test statistics	Further details
Cumulative parasite density	$F_{(1,8)} = 0.59$; P = 0.464	Wild type infections: 1.04 ±0.15 *pbmif*-ko1 infections: 0.68 ±0.16
Peak parasitaemia	$F_{(1,8)} = 5.00$; P = 0.056	Wild type infections: 7.24 ±1.03 *pbmif*-ko1 infections: 4.88 ±1.20
Minimum mass	$F_{(1,8)} = 3.04$; P = 0.119	Wild type infections: 17.74 ±0.53 *pbmif*-ko1 infections: 18.38 ±0.19
Minimum rbc density	$F_{(1,8)} = 0.20$; P = 0.668	Wild type infections: 8.00 ±0.29 *pbmif*-ko1 infections: 8.29 ±0.22
Cumulative reticulocyte density	***$F_{(1,8)} = 44.0$; P < 0.001***	Wild type infected hosts had significantly fewer reticulocytes (0.18 ±0.02) than *pbmif*-ko1 infected hosts (0.79 ±0.10)
Peak reticulocytaemia	***$F_{(1,8)} = 48.6$; P < 0.001***	Wild type infected hosts had significantly lower peak reticulocytaemia (1.02±0.07) than *pbmif*-ko1 infected hosts (3.32 ±0.45)

Table 1(b)

Variable	Test statistics	Further details
Cumulative parasite density	$F_{(1,7)} = 2.63$; P = 0.149	Wild type infections: 2.14 ±0.22 *pbmif*-ko1 infections: 1.72 ±0.15
Peak parasitaemia	$F_{(1,7)} = 3.86$; P = 0.091	Wild type infections: 14.83 ±1.78 *pbmif*-ko1 infections: 11.18 ±1.02
Minimum mass	$F_{(1,7)} = 2.75$; P = 0.142	Wild type infections: 17.07 ±0.44 *pbmif*-ko1 infections: 18.56 ±0.71
Minimum rbc density	$F_{(1,7)} = 1.26$; P = 0.299	Wild type infections: 6.93 ±0.46 *pbmif*-ko1 infections: 7.58 ±0.37
Cumulative reticulocyte density	***$F_{(1,7)} = 8.74$; P = 0.021***	Wild type infected hosts had significantly fewer reticulocytes (1.31 ±0.14) than *pbmif*-ko1 infected hosts (1.90 ±0.15)
Peak reticulocytaemia	***$F_{(1,7)} = 5.57$; P = 0.0503***	There is a borderline trend for the peak reticulocytaemia of wild type infected hosts (10.4 ±0.84) to be marginally higher than *pbmif*-ko1 infected hosts (8.12 ±0.63). However, mean reticulocyteamia was higher in *pbmif*-ko1 infected hosts on 3 of the 4 days measured. Therefore, this trend does not contradict the reticulocyte density result.

Table 2 (a)

Variable	Test statistics	Further details
Cumulative parasite density	***$F_{(2,12)} = 8.32$; $P = 0.005$***	Wild type parasites (0.13 ±0.04) did not reach significantly different densities to *pbmif*-ko1 parasites (0.28 ±0.09), but *pbmif*-ko2 parasites (0.76 ±0.16) reached significantly higher densities than both other genotypes. This does not show a consistent trend for *pbmif*-ko parasites to reach higher densities than wild type parasites.
Peak parasitaemia	$F_{(2,12)} = 0.06$; $P = 0.946$	Wild type infections: 12.90 ±2.32 *pbmif*-ko1 infections: 9.61 ±2.14 *pbmif*-ko2 infections: 11.74 ±2.59
Minimum mass	$F_{(2,12)} = 0.44$; $P = 0.653$	Wild type infections: 17.57 ±0.38 *pbmif*-ko1 infections: 17.05 ±0.44 *pbmif*-ko2 infections: 16.73 ±0.87
Mass loss	$F_{(2,12)} = 0.11$; $P = 0.901$	Wild type infections: 3.33 ±0.52 *pbmif*-ko1 infections: 3.08 ±0.84 *pbmif*-ko2 infections: 2.87 ±0.67
Minimum rbc density	$F_{(2,12)} = 0.18$; $P = 0.835$	Wild type infections: 5.07 ±0.43 *pbmif*-ko1 infections: 5.04 ±0.23 *pbmif*-ko2 infections: 4.79±0.39
Rbc loss	$F_{(2,12)} = 0.14$; $P = 0.871$	Wild type infections: 5.21 ±0.84 *pbmif*-ko1 infections: 4.91 ±0.29 *pbmif*-ko2 infections: 5.36 ±0.54
Cumulative reticulocyte density	***$F_{(2,12)} = 17.69$; $P < 0.001$***	Wild type infected hosts had significantly fewer reticulocytes (1.13 ±0.07) than *pbmif*-ko1 (2.51 ±0.25) and *pbmif*-ko2 infected hosts (2.28 ±0.15)
Peak reticulocytaemia	***$F_{(2,12)} = 24.00$; $P < 0.001$***	Wild type infected hosts had significantly lower peak reticulocytes (2.10 ±0.22) than *pbmif*-ko1 (4.24 ±0.35) and *pbmif*-ko2 infected hosts (5.56 ± 0.57)

Table 2 (b)

Variable	Test statistics	Further details
Cumulative parasite density	$F_{(2,12)} = 0.95$; $P = 0.415$	Wild type infections: 0.67 ±0.15 *pbmif*-ko1 infections: 0.50 ±0.10 *pbmif*-ko2 infections:0.79 ±0.19
Peak parasitaemia	$F_{(2,12)} = 1.93$; $P = 0.188$	Wild type infections: 6.48 ±1.54 *pbmif*-ko1 infections: 5.18 ±1.27 *pbmif*-ko2 infections: 10.36 ±2.70
Minimum mass	$F_{(2,12)} = 1.97$; $P = 0.182$	Wild type infections: 16.42 ±0.42 *pbmif*-ko1 infections: 16.53 ±0.46 *pbmif*-ko2 infections: 16.41 ±0.30
Mass loss	$F_{(2,12)} = 0.03$; $P = 0.975$	Wild type infections: 0.34 ±0.17 *pbmif*-ko1 infections: 0.82 ±0.15 *pbmif*-ko2 infections: 0.94 ±0.32

Minimum rbc density	***$F_{(2,12)} = 11.84; P = 0.001$***	*pbmif*-ko2 infected were more anaemic (4.74 ±0.29) than wild type infected hosts (7.27 ±0.35). *pbmif*-ko1 infected hosts (5.86 ±0.43) did not reach significantly different minimum red cell densities than wild type infected hosts. Therefore, there is not a consistent trend for *pbmif*-ko infected hosts to be less anaemic than wild type infected hosts.
Rbc loss	$F_{(2,12)} = 2.28$; P = 0.102	Wild type infections: 2.33 ±0.20 *pbmif*-ko1 infections: 2.75 ±0.84 *pbmif*-ko2 infections: 4.15 ±0.48
Cumulative reticulocyte density	***$F_{(2,12)} = 8.61; P = 0.005$***	Wild type infected hosts had significantly fewer reticulocytes (0.41 ±0.10) than *pbmif*-ko1 (1.57 ±0.30) and *pbmif*-ko2 infected hosts (1.36 ±0.18)
Peak reticulocytaemia	***$F_{(2,12)} = 7.93; P = 0.006$***	Wild type infected hosts had significantly lower peak reticulocytes (2.20 ±0.58) than *pbmif*-ko1 (10.07 ±2.35) and *pbmif*-ko2 infected hosts (9.23 ± 1.77)

A

```
Human   MPMFIVNTNVPR-ASVPDGFLSELTQQLAQATGKPPQYIAVHVVPDQLMAFGGSSEPCALCSLHSIGKIG 69
Mouse   MPMFIVNTNVPR-ASVPEGFLSELTQQLAQATGKPAQYIAVHVVPDQLMTFSGTNDPCALCSLHSIGKIG 69
Bm-1    MPYFTIDTNIPQ-NSISSAFLKKASNVVAKALGKPESYVSIHVNGGQAMVFGGSEDPCAVCVLKSIGCVG 69
Pb      MPCCELITNISIPDDKAQNTLSEIEDAISNILGKPVAYIMSNYDYQKNLRFSGSNEGYCFVRLTSIGGIN 70
Pf      MPCCEVITNVNLPDDNVQSTLSQIENAISDVMGKPLGYIMSNYDYQKNLRFGGSNEAYCFVRITSIGGIN 70
Bm-2    MPLITLASNVPA-SRFPSDFNVQFTELMAKMLGKPTSRILLLVMPNAQLSHGTTENPSCFTVVKSIGSFS 69
        **   : :*:      .    :  : ::.  ***   :         : .. :.:   ..  : *** ..

Human   GAQNRSYSKLLCGLLAERLRISPDRVYINYYDMNAANVGWNNSTFALE-- 117
Mouse   GAQNRNYSKLLCGLLSDRLHISPDRVYINYYDMNAANVGWNGSTFA---- 115
Bm-1    PKVNNSHAEKLYKLLADELKIPKNRCYIEFVDIEASSMAFNGSTLG---- 115
Pb      RSNNSLLADKITKILSNHLSVKPRRVYIEFRDCSAQNFAFSGSLFG---- 116
Pf      RSNNSALADQITKLLVSNLNVKSRRIYVEFRDCSAQNFAFSGSLFG---- 116
Bm-2    ADKNIEYSSLISEFMKKTLDIDPAHCIIHFLNLDPENVGCNGTTMKELMK 119
           *   :. :  :: . * :   :  : : :..... ..: :
```

B

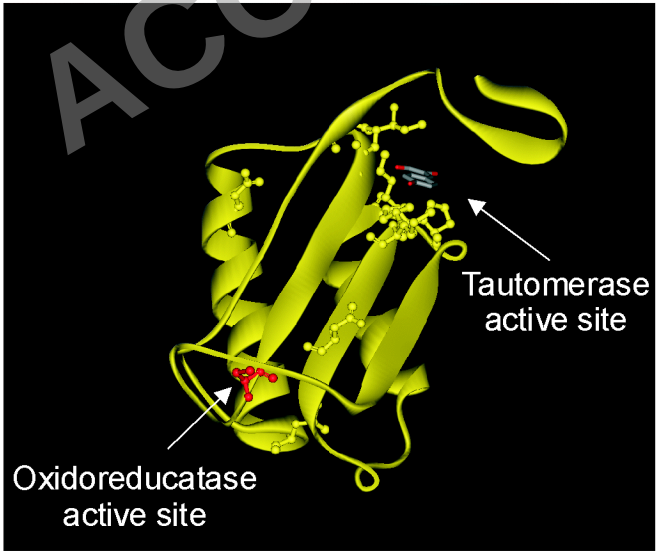

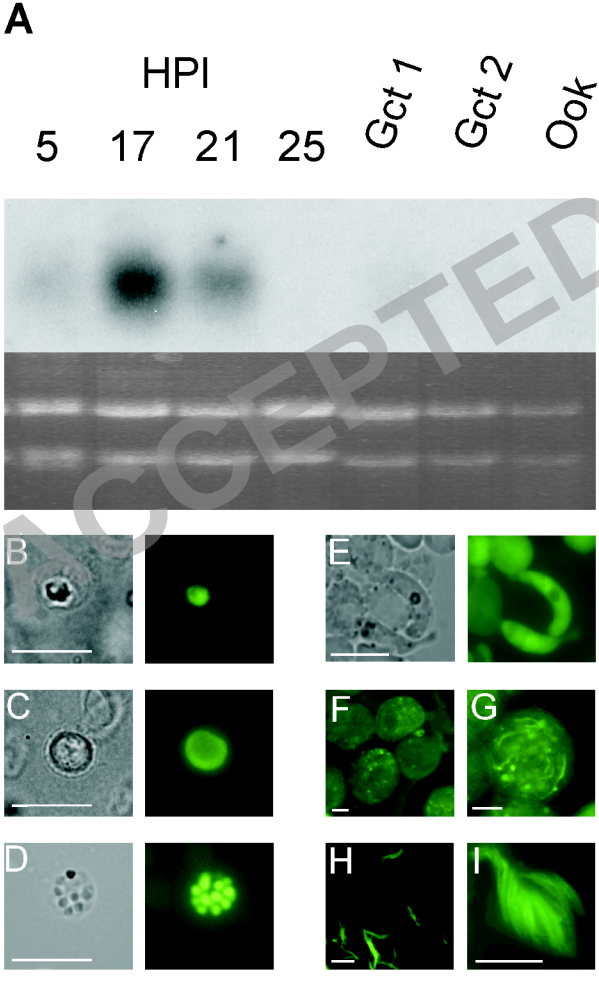

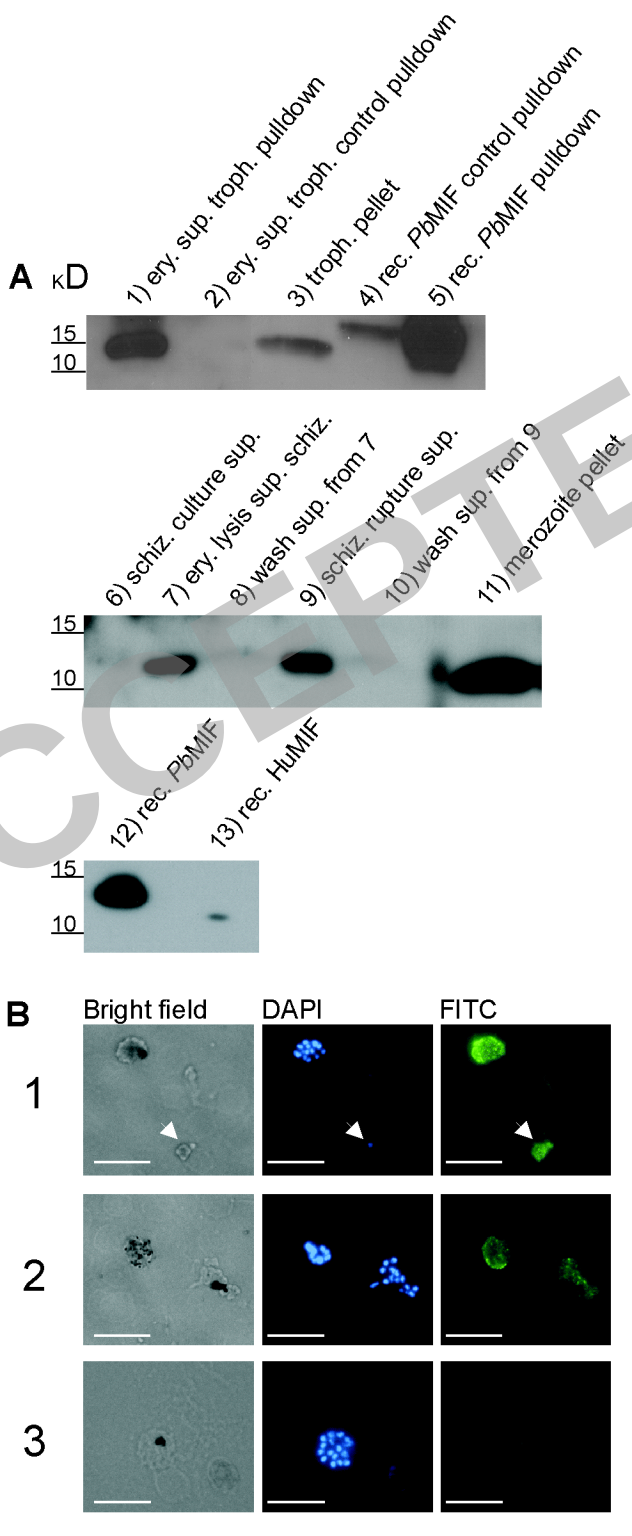
A
kD
1) ery. sup. troph. pulldown
2) ery. sup. troph. control pulldown
3) troph. pellet
4) rec. PbMIF control pulldown
5) rec. PbMIF pulldown
15
10
6) schiz. culture sup.
7) ery. lysis sup. schiz.
8) wash sup. from 7
9) schiz. rupture sup.
10) wash sup. from 9
11) merozoite pellet
15
10
12) rec. PbMIF
13) rec. HuMIF
15
10
B
Bright field
DAPI
FITC
1
2
3

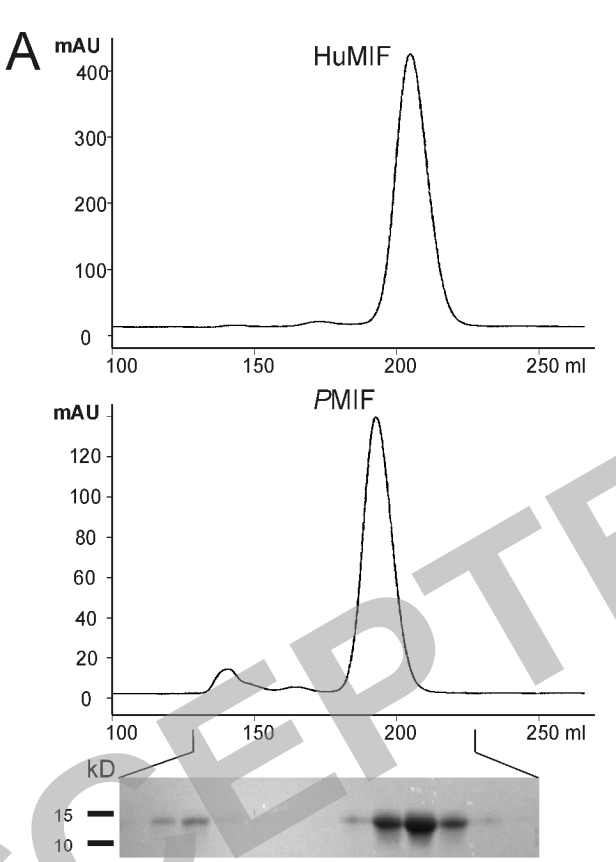
A
mAU
400
300
200
100
0
HuMIF
100
150
200
250 ml
mAU
120
100
80
60
40
20
0
PMIF
100
150
200
250 ml
kD
15
10

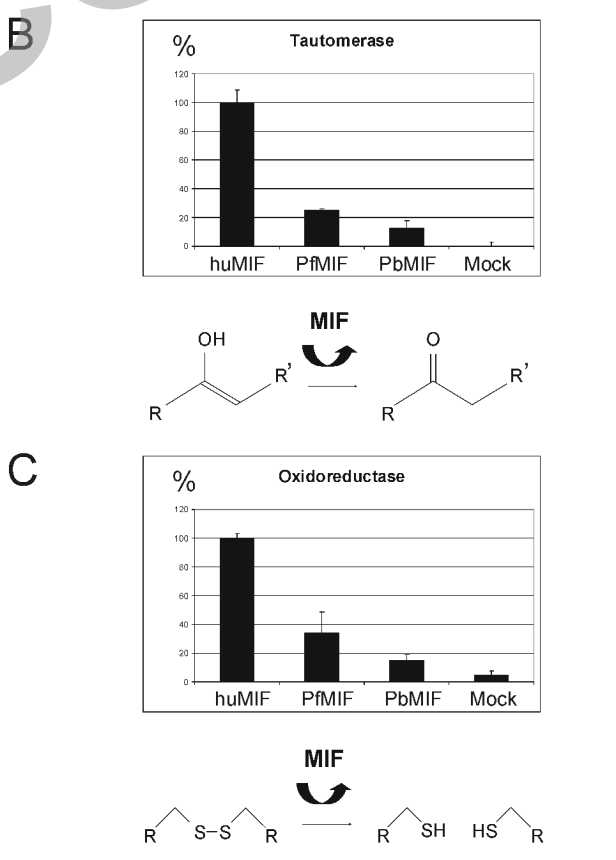
B
%
Tautomerase
120
100
80
60
40
20
0
huMIF
PfMIF
PbMIF
Mock
MIF
OH
R'
R
O
R'
R
C
%
Oxidoreductase
120
100
80
60
40
20
0
huMIF
PfMIF
PbMIF
Mock
MIF
R
S–S
R
R
SH
HS
R

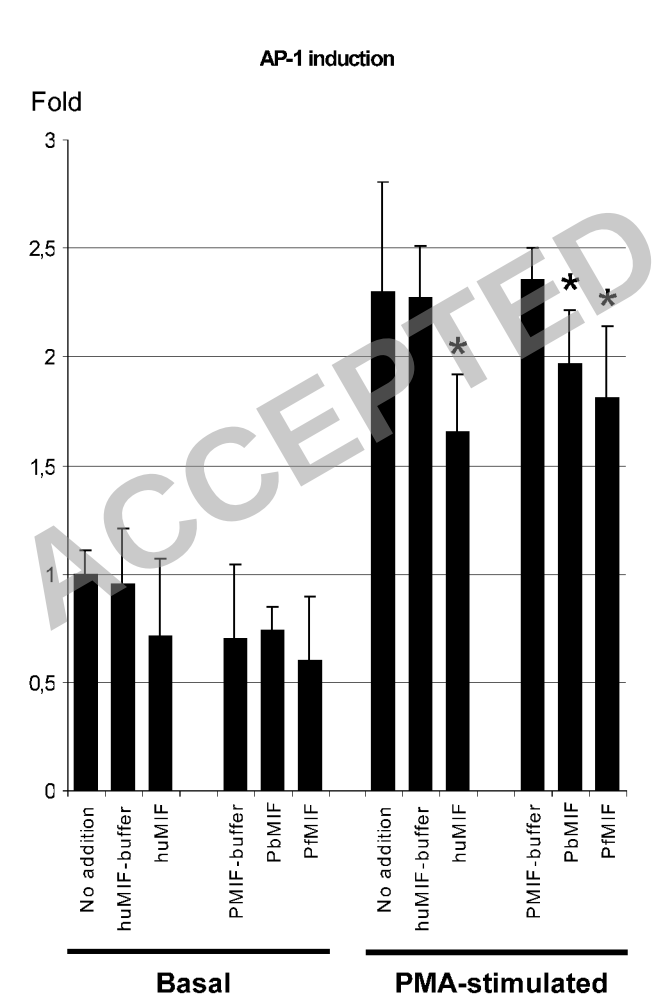
AP-1 induction
Fold
3
2,5
2
1,5
1
0,5
0
No addition
huMIF-buffer
huMIF
PMIF-buffer
PbMIF
PfMIF
No addition
huMIF-buffer
huMIF
PMIF-buffer
PbMIF
PfMIF
Basal
PMA-stimulated
*
*
*

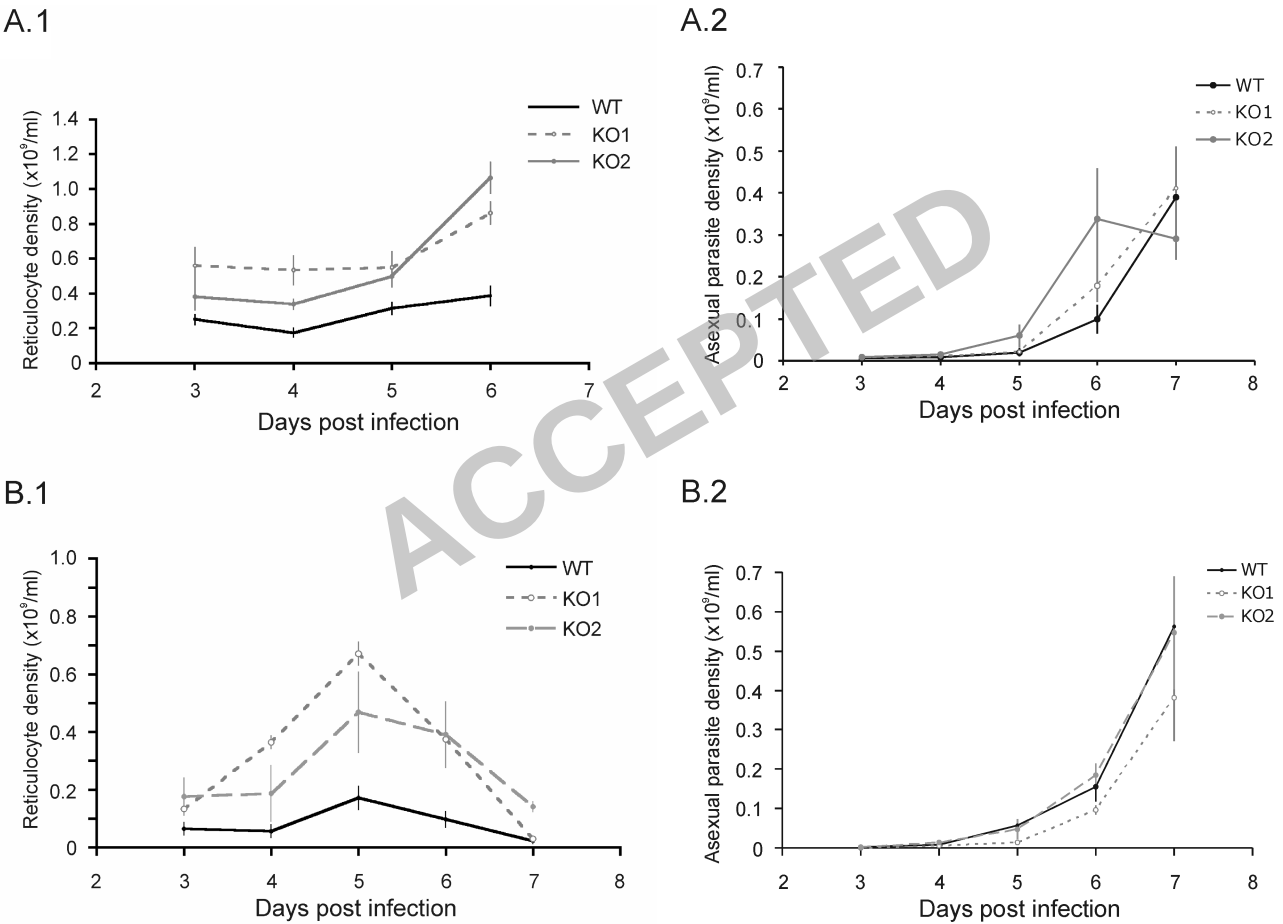
A.1
Reticulocyte density (x10⁹/ml)
1.4
1.2
1.0
0.8
0.6
0.4
0.2
0
2
3
4
5
6
7
Days post infection
WT
KO1
KO2
A.2
Asexual parasite density (x10⁹/ml)
0.7
0.6
0.5
0.4
0.3
0.2
0.1
0
2
3
4
5
6
7
8
Days post infection
WT
KO1
KO2
B.1
Reticulocyte density (x10⁹/ml)
1.0
0.8
0.6
0.4
0.2
0
2
3
4
5
6
7
8
Days post infection
WT
KO1
KO2
B.2
Asexual parasite density (x10⁹/ml)
0.7
0.6
0.5
0.4
0.3
0.2
0.1
0
2
3
4
5
6
7
8
Days post infection
WT
KO1
KO2

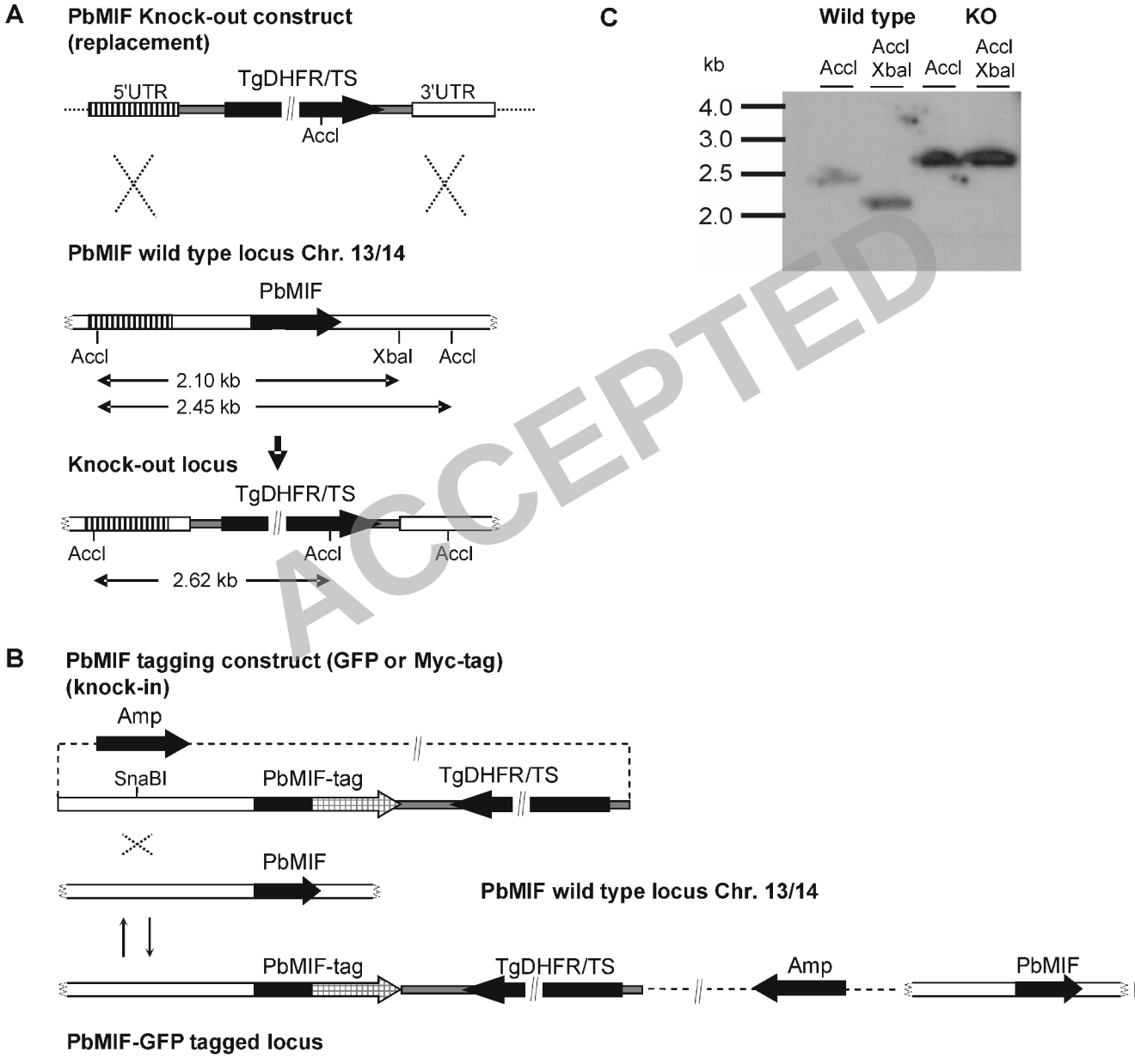
A
PbMIF Knock-out construct
(replacement)
5'UTR
TgDHFR/TS
3'UTR
AccI
PbMIF wild type locus Chr. 13/14
PbMIF
AccI
XbaI
AccI
2.10 kb
2.45 kb
Knock-out locus
TgDHFR/TS
AccI
AccI
AccI
2.62 kb
C
Wild type
KO
kb
AccI
AccI XbaI
AccI
AccI XbaI
4.0
3.0
2.5
2.0
B
PbMIF tagging construct (GFP or Myc-tag)
(knock-in)
Amp
SnaBI
PbMIF-tag
TgDHFR/TS
PbMIF
PbMIF wild type locus Chr. 13/14
PbMIF-tag
TgDHFR/TS
Amp
PbMIF
PbMIF-GFP tagged locus